

RSC Advances



This is an *Accepted Manuscript*, which has been through the Royal Society of Chemistry peer review process and has been accepted for publication.

Accepted Manuscripts are published online shortly after acceptance, before technical editing, formatting and proof reading. Using this free service, authors can make their results available to the community, in citable form, before we publish the edited article. This *Accepted Manuscript* will be replaced by the edited, formatted and paginated article as soon as this is available.

You can find more information about *Accepted Manuscripts* in the [Information for Authors](#).

Please note that technical editing may introduce minor changes to the text and/or graphics, which may alter content. The journal's standard [Terms & Conditions](#) and the [Ethical guidelines](#) still apply. In no event shall the Royal Society of Chemistry be held responsible for any errors or omissions in this *Accepted Manuscript* or any consequences arising from the use of any information it contains.

**DNA-Capped Fe₃O₄/SiO₂ Magnetic Mesoporous Silica Nanoparticles for
Potential Controlled Drug Release and Hyperthermia**

Yufang Zhu^{a*}, Cuilian Tao^b

^aSchool of Materials Science and Engineering, University of Shanghai for Science and
Technology, 516 Jungong Road, Shanghai, 200093, China.

^bSchool of Medical Instrument and Food Engineering, University of Shanghai for
Science and Technology, 516 Jungong Road, Shanghai, 200093, China.

*Corresponding authors: Prof. Yufang Zhu

Tel: +86-21-55271663;

Email: zjf2412@163.com

Abstract: We proposed a strategy to construct DNA-capped $\text{Fe}_3\text{O}_4/\text{SiO}_2$ magnetic mesoporous silica (MMS) nanoparticles for potential temperature controlled drug release and magnetic hyperthermia. Drug release behavior, magnetic heating capacity, in vitro cytotoxicity, and cell uptake of the MMS-based nanocarriers were evaluated. The results showed that the DOX/MMS-NH₂-dsDNA complexes could release DOX fast at 50 °C, but very slow at 37 °C. Also, MMS-based nanocarriers could efficiently generate heat upon exposure to an alternating magnetic field due to the superparamagnetic behavior. Furthermore, the MMS-NH₂-dsDNA complexes could be effectively taken up by murine breast cancer 4T1 cells, and negligible cytotoxicity of the MMS-NH₂-dsDNA complexes has been observed. Therefore, DNA-capped MMS nanoparticles had potential for cancer therapy with temperature controlled drug release and magnetic hyperthermia.

Keywords: Magnetic mesoporous silica, Controlled release, Hyperthermia, DNA capping

1. Introduction

Controlled drug release systems are of great important in drug delivery. To date, various organic and inorganic carriers have been investigated for controlled drug release systems [1]. Among inorganic carriers, biocompatible and biodegradable hydroxyapatite (HA) nanoparticles have been widely studied for drug delivery, and HA nanoparticles showed great potential as drug carriers with high drug loading and pH-responsive features for future intracellular drug delivery system [2-6]. Mesoporous silica nanoparticles (MSN) are another promising candidate carriers for drug delivery due to their high surface area, large pore volume, good biocompatibility and ease of surface functionalization [7-9]. In particular, the readily functionalized surface allows MSN to construct smart caps on the mesopore outlets to control their opening or closing state, resulting in the controlled drug release. Many studies have reported the design of smart caps, such as nanoparticles, cyclodextrin, gelatin, supramolecular assemblies and biomolecules, to control drug release from MSN in response to different stimuli including light, pH, temperature, redox activation, competitive binding and enzymes [10-18].

Temperature is an external stimulus and provides a great opportunity to release a drug at a desired time. For example, Fu et al., Zhou et al. and You et al. reported the temperature-responsive controlled release systems based on poly(N-isopropylacrylamide) (PNIPAM)-modified MCM-41 and mesostructure cellular foam materials (MCFs) [19-21]. Jiao et al. prepared the copolymer of 2-(2-methoxyethoxy)ethyl methacrylate (MEO₂MA) and oligo(ethylene glycol)

methacrylate (OEGMA) cross-linked by disulfide bonds (P(MEO₂MA-*s-s*-OEGMA)) to coat hollow MSN, and found that the loaded drugs could be released rapidly at a temperature higher than 37 °C [22]. However, these temperature-controlled drug release systems showed the complicated synthesis and coating process of the temperature-responsive polymers on MSN. Also, Aznar et al. and Liu et al. designed temperature-controlled drug release systems based on MSN with phase-change molecules as caps [23-24], but the limited phase-change molecules could be used to construct the controlled drug release systems due to the requirements of biocompatibility, biosafety and phase-change temperature in the range of body temperature.

Recently, DNA-capped MSN as the controlled release nanocarriers have attracted more attention due to the easy synthesis and programmability, good biocompatibility and high cellular uptake [25-34]. Most important, DNA molecules as caps could response to many stimuli, such as temperature, pH, enzyme and competitive binding [25-34]. For example, Chen et al. used i-motif quadruplex DNA to cap the mesopores and triggered pH-controlled release based on the morphology change of DNA chains [26]. Zhu et al. reported an enzyme-triggered drug release system that is based on CpG oligodeoxynucleotide-capped hollow mesoporous silica particles [34]. Zhang et al. developed a nanocarrier by capping MSN with a programmable DNA hybrid, and the drug release was controlled by microRNA owing to the competitive binding [18]. From the viewpoint of practical application, these methods to trigger drug release with the stimuli of pH, enzyme and competitive

binding are challenging because of the complexity of the in vivo environment.

However, the temperature-responsive controlled drug release from DNA-capped MSN is promising for clinical applications. On one hand, the DNA duplex endows the feature with temperature tunability in the range of body temperature through changes in chain length, variations in G/C content, or even the size and surface density of oligonucleotides attached to the nanoparticles [31,35]. On the other hand, many possible stimuli, such as near-infrared (NIR) light and magnetic field can trigger the DNA-capped MSN-based nanocarriers to generate heat for the uncapping of mesopores, and thereby release drugs [31-33]. For example, Chang et al. and Li et al. developed NIR light-triggered nanocarriers for controlled drug release, in which the drugs can be loaded into mesoporous silica coated Au nanorods and then capped with DNA [32-33], because Au nanorods with strong surface plasmon resonance are highly absorbent of light in the NIR region and can act as a nanoheater by absorbing the NIR laser. However, the practical application of light-triggered drug delivery systems could be limited due to the low tissue penetration depth of light (several mm for NIR light) [36].

In comparison, human tissues are transparent to the magnetic field, thus the use of a magnetic field can serve as an alternative approach to overcome the limitation of low tissue penetration depth of light [37]. On one hand, magnetic mesoporous nanoparticles can generate heat under an alternating magnetic field due to the Néel and Brownian relaxation or hysteresis loss of magnetic nanoparticles [38], which can induce the DNA-capped magnetic mesoporous nanoparticles to

denaturize the DNA capping. For example, Ruiz-Hernandez et al. conjugated double-stranded DNA (dsDNA) together with spherical $\gamma\text{-Fe}_2\text{O}_3$ magnetic nanoparticles to cap the mesopores of MSN, and utilized a magnetic field to induce heat for triggering the uncapping of mesopores for drug release [31]. On the other hand, magnetic hyperthermia, a type of cancer therapy in which body tissue is exposed to magnetic field for increasing the temperature to be higher than normal body temperature ($\approx 41\text{-}46\text{ }^\circ\text{C}$), has been developed as an efficacious treatment modality for localized or deeply exist cancer [39-43]. Moreover, magnetic hyperthermia could combine chemotherapy to improve cancer therapeutic efficiency, because hyperthermia can render tumor cells temporarily more sensitive to anticancer drugs [44]. Therefore, it can be imagined that DNA-capped magnetic mesoporous silica (MMS) nanoparticles could be a promising multifunctional platform for potential cancer therapy with temperature controlled drug release and hyperthermia under an alternating magnetic field. That is to say, after the DNA-capped MMS nanoparticles-based drug delivery system arrive the tumor sites, the heat will be generated from MMS nanoparticles to raise the temperature of the surrounding tumor organ/cells for hyperthermia therapy when applied an alternating magnetic field. At the same time, the generated heat increases the temperature of the DNA-capped MMS nanocarrier, resulting in the opening of the mesopores to release drugs for chemotherapy.

Herein we proposed a concept to develop DNA-capped $\text{Fe}_3\text{O}_4/\text{SiO}_2$ MMS nanoparticles as nanocarriers for potential temperature controlled drug release and

hyperthermia. As shown in Fig. 1, Fe_3O_4 nanoparticles were prepared and incorporated into mesoporous silica matrix to form $\text{Fe}_3\text{O}_4/\text{SiO}_2$ MMS nanoparticles. MMS nanoparticles are functionalized with single-stranded DNA (ssDNA) through the modification of amino groups on MMS nanoparticles and the grafting of 6-Maleimidocaproic acid sulfo-N-succinimidyl ester (sulfo-EMCS) linkers with amino groups. After loading of doxorubicin (an anticancer drug), ssDNA functionalized MMS nanoparticles are capped with complementary ssDNA (cDNA) through the formation of double-stranded DNA (dsDNA) for capping the mesopores. When applied an alternating magnetic field, the DNA-capped MMS nanoparticles generate heat for hyperthermia, and the loaded drugs could be simultaneously released by the heat-triggered denaturation of the dsDNA capping chains.

2. Experimental

2.1 Materials:

Tetraethyl orthosilicate (TEOS), triethanolamine (TEA), ethanol, hydrochloride Acid(HCl, 37%), potassium dihydrogen phosphate (KH_2PO_4), sodium hydroxide (NaOH), ferric chloride ($\text{FeCl}_3 \cdot 6\text{H}_2\text{O}$), ferrous chloride ($\text{FeCl}_2 \cdot 4\text{H}_2\text{O}$) were obtained from Sinopharm Chemical Reagent Co. Ltd., PBS (pH 7.4), HEPES buffer, doxorubicin hydrochloride (DOX), and EDTA disodium salt dihydrate were obtained from Sangon Biotech (Shanghai) Co. Ltd., Hexadecyltrimethylammonium p-toluenesulfonate (CTAT) and 3-aminopropyltriethoxysilane (APTES) were obtained from Sigma-Aldrich. 6-Maleimidocaproic acid sulfo-N-succinimidyl ester (sulfo-EMCS) was purchased from

Toronto Research chemicals Inc. Ultrapure water was obtained from Millipore pure water system. All chemicals were of analytical-reagent grade and used without further purification. Oligonucleotides were purchased from Sangon Biotech (Shanghai) Co. Ltd., and the sequences are 5'-SH(CH₂)₆TTATCGCTG ATTCAA-3' (ssDNA) and 5'-TTGAATCAGCGATAATCGAATAGCGACTAAGTT-3' (cDNA).

2.2 Synthesis of aminated magnetic mesoporous silica nanoparticles (MMS-NH₂)

MMS nanoparticles were synthesized according to the previously reported method [45]. Amino groups were grafted onto MMS nanoparticles to form MMS-NH₂ nanoparticles as follows: 0.5 g of MMS nanoparticles was homogeneously dispersed in 100 ml ethanol and sonicated for 30 min. Subsequently, 1.5 ml of APTES was added to the suspension with mild stirring for 24 h at the room temperature. The suspension was filtered off and washed extensively with ethanol to remove the residual APTES. Finally, the MMS-NH₂ nanoparticles were dried in vacuum at 50 °C for 12 h.

2.3 Characterization

The wide angle X-ray diffraction (WAXRD) patterns were obtained on a D8 ADVANCE powder diffractometer using Cu K α 1 radiation (1.5405 Å). Transmission electron microscopy (TEM) images were obtained using a JEM-2100F transmission electron microscope at an acceleration voltage of 200 kV. N₂ adsorption–desorption isotherms were obtained on a Micromeritics Tristar 3020 automated surface area and pore size analyzer at –196 °C under continuous adsorption conditions. Brunauer–Emmett–Teller (BET) and Barrett–Joyner–Halenda (BJH) methods were

used to determine the surface area and mesopore size distribution. Zeta potential measurements were performed on a Malvern zeta sizer Nano-ZS90. Fourier transform infrared (FTIR) spectra were recorded on a LAM750(s) spectrometer in transmission mode. UV–Vis analysis was measured on a Nanodrop 2000C spectrophotometer. Magnetization curve was carried out using a TF-WI-ZDYP V 3.0.4 vibrating sample magnetometer (VSM) at 298 K.

2.4 Functionalization of MMS-NH₂ with ssDNA (MMS-ssDNA)

5'-SH(CH₂)₆TTATCGCTGATTCAA-3' (ssDNA) coupling to MMS-NH₂ nanoparticles was performed using sulfo-EMCS as a cross-linker according to the reported method [33]. Typically, 10 mg of MMS-NH₂ nanoparticles was first dispersed to 950 µl of HEPES buffer (20 Mm, pH 7.0) by ultrasonication for 10 min. Subsequently, the suspension was reacted with 50 µl of sulfo-EMCS for 1 h, and the sulfo-EMCS linked nanoparticles were isolated by centrifugation and washed with hybridization buffer. To functionalize nanoparticles with ssDNA, the sulfo-EMCS linked nanoparticles were dispersed into another 950 ul of HEPES buffer, following by the addition of 30 µl of ssDNA (1 mmol/l). The suspension was shaken at room temperature for 3 h. Finally, the ssDNA-functionalized MMS-NH₂ (MMS-ssDNA) nanoparticles were filtered off and washed with hybridization buffer to remove the residual ssDNA.

2.5 Drug loading and complementary ssDNA (cDNA) capping (DOX/MMS-dsDNA)

DOX, an anticancer drug, was loaded into mesopores by soaking the obtained MMS-ssDNA nanoparticles into 1 ml of DOX solution (0.5 mol/l in HEPES buffer) under dark conditions at the room temperature for 24 h. Subsequently, 30 µl of

complementary ssDNA (5'-TTGAATCAGCGATAATCGAATAGCGACTAAGTT-3', 1mmol/l) was added in the mixture with continuous stirring for another 3 h to allow the hybridization. The DOX/MMS-dsDNA complexes were collected by centrifugation at 12000 rpm for 10 min and washed extensively with hybridization buffer to remove the residual DOX and cDNA. The supernatant was collected for UV-vis analysis at the wavelength of 488 nm to estimate the DOX loading capacity.

2.6 DOX release from the DOX/MMS-dsDNA complexes

In vitro release of DOX from the DOX/MMS-dsDNA complexes was carried out in the release solution of pH7.4 or pH5.0 with shaking at 100 rpm. The temperature of the release solution was kept at 37 °C or 50 °C. DOX release from the DOX/MMS-dsDNA complexes in the release solution of pH7.4 at 37 °C as an example: the obtained DOX/MMS-dsDNA complexes were dispersed into 1 ml of PBS solution with pH 7.4 at 37 °C. At predetermined time intervals, the release system was centrifuged and 20 µl of the supernatant solution was taken out for UV-Vis analysis to determine the released DOX amount, and replaced with the same amount of fresh medium each time. Before determination, a calibration curve was recorded by measuring the absorbance values at the absorbance of DOX at 488 nm.

2.7 Magnetic heating capacity of MMS-NH₂ nanoparticles

The magnetic heating capacity of MMS-NH₂ nanoparticles were evaluated using a DM100 System (NanoScale Biomagnetics, Spain) and the temperature was measured with an optical fiber temperature sensor. MMS-NH₂ nanoparticles were dispersed in water to a concentration of 50 mg/ml. The suspension was heated

under an alternating magnetic field with the strength of 90–180 Gauss and the frequency of 409 kHz for 20 min, respectively. The upper limit of temperature was set to be 80 °C. The capacity of MMS-NH₂ nanoparticles to absorb energy from an alternating magnetic field is quantified by the specific absorption rate (SAR).

2.8 Cell culture

Murine breast cancer 4T1 cells were maintained in RPMI-1640 medium containing 10% fetal bovine serum, 100 units/mL penicillin, and 100 mg/mL streptomycin. Cells were cultured with the complete medium in 5% CO₂ at 37°C. For all experiments, cells were harvested from sub-confluent cultures by the use of trypsin and were resuspended in fresh complete medium before plating.

2.9 In vitro cytotoxicity assay

An in vitro cytotoxicity assay for MMS nanoparticles was using a 3-[4,5-dimethylthiazol-2-yl]-2,5-diphenyltetrazolium bromide (MTT) assay. 4T1 cells were seeded into a 96-well plate at a density of 1×10^4 cells per well. After seeding the cells, the MMS-dsDNA complexes solution (1 mg/ml in RPMI-1640 medium) was immediately added into a 96-well plate. The final concentrations of the MMS-dsDNA complexes were 0, 25, 50, 75, 100 and 200 µg/ml, and the final medium volume in each well was 100 µl. After incubation of cells for 24 h, the medium containing the MMS-dsDNA complexes was removed, and 10 µl of MTT solution was added to each well. After incubation at 37°C for another 4 h, 100 µl of dimethyl sulfoxide (DMSO) was added to each well to dissolve the pure formazan crystal. Then, the plates were

read at 570 nm using a microplate reader (MK3, Thermo). The cytotoxicity was expressed as the percentage of cell viability compared to the untreated control cells.

2.10 Cell uptake assay

For investigation on cell uptake of the MMS-dsDNA complexes, the cDNA was labeled with FITC to hybridize with ssDNA to form the MMS-dsDNA –FITC complexes. In a typical procedure, coverslips with a diameter of 14 mm were pretreated with 5% HCl, 30% HNO₃, and 75% alcohol and then fixed in a 12-well tissue culture plate. 5×10^4 4T1 cells were seeded into each well and cultured for about 48 h to allow the 4T1 cells to attach onto the coverslip. After the cells were washed twice with PBS, the MMS-dsDNA-FITC complexes were added to each well in a concentration of 100 µg/ml. After incubation for 6 h, the 4T1 cells were fixed with glutaraldehyde (4 %) for 15 min at 4 °C and stained with DAPI (1 µg/mL) for 15 min at 4 °C using a standard procedure. Finally, the samples were imaged using a 63× oil-immersion objective lens on a confocal laser scanning microscopy (Carl Zeiss LSM 700, Jena, Germany).

3. Results and discussion

3.1 Characterization of MMS-NH₂ nanoparticles

Preparation of MMS-NH₂ nanoparticles involved the incorporation of Fe₃O₄ nanoparticles into mesoporous silica matrix with hexadecyltrimethylammonium p-toluenesulfonate as structure-directing agent [46] and the functionalization of amino groups onto the surface of MMS nanoparticles through the grafting method using 3-aminopropyltriethoxysilane. As shown in Fig. 2A, a broad reflection at 2θ

$\approx 20-25^\circ$ is attributed to the amorphous mesoporous silica matrix, and other well-resolved diffraction peaks can be indexed to Fe_3O_4 phase according to the reflection peak positions and relative intensities. The magnetization curve of the MMS- NH_2 nanoparticles shows a very small hysteresis loop with the coercivity of 3.5 Oe and the remanence of 0.2 emu/g, suggesting the superparamagnetic behavior of MMS- NH_2 nanoparticles (Fig. 2B). The saturation magnetization value is estimated to be 4.2 emu/g. Therefore, MMS- NH_2 nanoparticles have potential to generate heat under alternating magnetic field due to their superparamagnetic behavior. TEM image shows that MMS- NH_2 nanoparticles are spherical and highly monodisperse, and the particle sizes are estimated to be about 100-200 nm (Fig. 2C). Moreover, Fe_3O_4 nanoparticles are embedded in each MMS- NH_2 nanoparticle, and the mesopores can be clearly observed on MMS- NH_2 nanoparticles. N_2 adsorption-desorption measurement shows a typical type IV isotherm, indicative of a mesoporous structure. The BET surface area and the pore volume are found to be about $372 \text{ m}^2/\text{g}$ and $1.44 \text{ cm}^3/\text{g}$, respectively. The BJH pore sizes are mainly distributed in 2-4 nm. It suggested that the mesoporous channels and high surface area allow drug molecules to load in MMS- NH_2 nanoparticles.

On the other hand, FTIR spectra and zeta potential were used to verify the grafting of amino groups onto the surface of MMS nanoparticles. As shown in Fig. 3, After MMS were modified with amino groups, vibration peaks can be observed at 1340 and 1385 cm^{-1} assigned to the stretching bands of C-N groups, and the peaks at 1495 and 1560 cm^{-1} can be attributed to the bending vibration of N-H groups. At the

same time, the Si-OH band at 960 cm^{-1} in the MMS spectrum became significantly weaker after modifying with amino groups. These results indicated that amino groups have been modified onto MMS nanoparticles. Zeta potential measurements further confirmed the amino modification of MSN. As shown in Fig. 4, zeta potential value of the nanoparticles was reversed from a negative value of $-14.88 \pm 0.19\text{ mV}$ to a positive one of $6.09 \pm 0.25\text{ mV}$ due to the grafting of 3-aminopropyltriethoxysilane, suggesting the grafting of positively charged amino groups onto the surface of MMS nanoparticles to form MMS-NH₂ nanoparticles.

3.2 Preparation of the DOX/MMS-NH₂-dsDNA complexes and the temperature controlled DOX release behavior

For capping the mesopore outlets of MMS-NH₂ nanoparticles with dsDNA, 15-mer ssDNA was firstly conjugated onto the surface of MMS-NH₂ nanoparticles to form MMS-NH₂-ssDNA complexes by using sulfo-EMCS linkers. As shown in Fig. 4, zeta potential value of the MMS-NH₂-ssDNA complexes decreased from $6.09 \pm 0.25\text{ mV}$ to $-6.32 \pm 0.03\text{ mV}$ due to the conjugation of negative charged ssDNA on MMS-NH₂ nanoparticles. On the other hand, the appearance of a minor peak at 2510 cm^{-1} in the FTIR spectrum of the MMS-NH₂-ssDNA complexes also suggests the successful conjugation of the SH-labeled ssDNA on MMS-NH₂ nanoparticles.

To investigate temperature controlled drug release, we used anti-cancer drug, doxorubicin (DOX), as a model drug to introduce into MMS-NH₂-ssDNA complexes, and then cap the mesoporous outlets through the hybridization of 33-mer

complementary ssDNA (cDNA) with the 15-mer ssDNA chain on the MMS surface. As shown in Fig. 4, zeta potential value further decreased to -16.27 ± 0.22 mV owing to the hybridization of 33-mer cDNA with 15-mer ssDNA. The loaded amount of DOX in the DOX/MMS-NH₂-dsDNA complexes was estimated to be ca. 40 μ g/mg MMS-ssDNA nanoparticles, which was determined from the difference in the DOX concentration between the initial solution and the residual supernatant using UV-vis analysis at the characteristic absorbance peak of DOX (488 nm) according to the Beer–Lambert law.

With the aim to verify the performance of dsDNA capping in response to changes in temperature, the DOX/MMS-NH₂-dsDNA complexes were dispersed into the release solution (pH 7.4 or pH5.0) at 37 or 50 °C, respectively, in order to investigate the drug release behavior. Fig. 5 shows the DOX release profiles of the DOX/MMS-NH₂-dsDNA complexes under different pH and temperature conditions. At the temperature of 37 °C, less than 7% DOX was released from the DOX/MMS-NH₂-dsDNA complexes in the release solution of pH 7.4, and only 17% DOX was released in the release solution of pH 5.0, which indicated that the dsDNA could cap the mesoporous outlets to prevent the DOX molecules from leaking effectively. While at the temperature of 50 °C, much more DOX were released from the DOX/MMS-NH₂-dsDNA complexes at both pH conditions. About 50% DOX was released from the DOX/MMS-NH₂-dsDNA complexes within 9 h in the release solution of pH 5.0, and about 27% DOX could be released from the complexes within 9 h in the release solution of pH 7.4. The results indicated that the

DOX/MMS-NH₂-dsDNA complexes exhibited temperature controlled drug release behavior due to the denaturation of the dsDNA capping chains at 50 °C, higher than the melting temperature of the dsDNA (40.3 °C) [29]. On the other hand, at the same temperature, the DOX release rate in the release solution of pH 5.0 was faster than that in the release solution of pH 7.4. It might be that DOX molecules were adsorbed on the mesopore surfaces of MMS-NH₂ nanoparticles via electrostatic interaction. When the pH value of the release solution decreased, the interaction forces between DOX and MMS-NH₂ nanoparticles could decrease due to the protonation of the aminated surfaces, resulting in easier detachment of DOX molecules and thereby increase the DOX release rate.

It has demonstrated that the pH environment of cancer cells was nearly pH 7.4, while that of the endosome/lysosome and cytosol in cells was estimated to be pH 5.0–5.5. Therefore, such a drug release behavior is very useful for an efficient drug delivery system, because the very slow DOX release at pH 7.4 and 37 °C could decrease the side effect of DOX release during the transport of the drug delivery system in bloodstream. While much faster DOX release occurs at acid pH and hyperthermia temperature after drug delivery system arrives at the targeted cancer cells, which could enhance the therapeutic efficiency. Therefore, dsDNA-capped MMS nanoparticles as carriers for DOX delivery had temperature controlled drug release behavior and would be beneficial for chemotherapy.

3.3 Magnetic heating capacity of MMS-NH₂ nanoparticles

The presence of magnetic Fe_3O_4 nanoparticles in mesoporous silica matrix ensures the potential of the MMS- NH_2 nanoparticles to reach hyperthermia temperature range under an alternating magnetic field. Fig. 6 shows the magnetic heating capacity of the MMS- NH_2 nanoparticles with a concentration of 50 mg/ml in H_2O evaluated under the magnetic field with a frequency of 409 kHz and magnetic field strength of 90-180 Gauss. From the temperature kinetic curves (Fig. 6A), the MMS- NH_2 nanoparticles can generate heat to increase the surrounding temperature. With the increase of magnetic field strength, the temperature increase became faster. The absolute temperature increases in 20 min was estimated to be 13.1, 21.2, 31.6 and 46.2 °C when the magnetic field strength was 90, 120, 150 and 180 Gauss, respectively (insert in Fig. 6A). Furthermore, the magnetic heating capacity of the MMS- NH_2 nanoparticles was quantified through the specific absorption rate (SAR). It can be found that the magnetic heating capacity of the MMS- NH_2 nanoparticles was dependent on the magnetic field strength. As shown in Fig. 6B, the SAR values increased with an increase of magnetic field strength. When magnetic field strength was increased from 90 to 180 Gauss, SAR value increased from 1.44 to 8.74 W/g. Martín-Saavedra et al. investigated the ability of magnetic mesoporous silica spheres to conduct magnetic hyperthermia upon exposure to an alternating magnetic field using cancer cells, and the results showed the ability to control the temperature rise in the cell culture environment after the treatment of magnetic mesoporous silica spheres under alternating magnetic field, and thereby induced the significant decrease in cell viability [47]. Therefore, the MMS- NH_2 -dsDNA complexes had

potential to apply for magnetic hyperthermia therapy, although the value of SAR should be as high as possible to minimize the amount of magnetic material applied for hyperthermia.

3.4 In vitro cytotoxicity and cell uptake of the MMS-NH₂-dsDNA complexes

Evaluation of the cytotoxicity of drug delivery carriers is important for drug delivery systems. In this study, In vitro cytotoxicity of the MMS-NH₂-dsDNA complexes to murine breast cancer 4T1 cells was evaluated using MTT assay. As shown in Fig. 7, after incubation of cells with the MMS-NH₂-dsDNA complexes for 24 h, cell viabilities did not show a significant difference even up to a concentration of 200 µg/ml compared to the control group, which indicated that the MMS-NH₂-dsDNA complexes had low cytotoxicity and could be used as carriers for DOX delivery.

It is desirable for drug carriers to be taken up by cancer cells. In this study, cell uptake of the MMS-NH₂-dsDNA complexes could facilitate local magnetic hyperthermia owing to magnetic heating in cancer cells. On the other hand, cell uptake of the MMS-NH₂-dsDNA complexes could also be beneficial for chemotherapy due to the enhancement of the intracellular delivery of DOX, and thereby enhancing the anticancer activity of DOX. To verify the cell uptake of the MMS-NH₂-dsDNA complexes, the MMS-NH₂-ssDNA nanoparticles hybridized with FITC-labeled 33-mer cDNA to form the MMS-NH₂-dsDNA-FITC complexes, and the MMS-NH₂-dsDNA-FITC complexes were incubated with 4T1 cells for 6 h. As shown in Fig. 8, green

fluorescence from the MMS-NH₂-dsDNA-FITC complexes were distributed in the cells and primarily located between cell membrane and nucleus, which suggest that the MMS-NH₂-dsDNA-FITC complexes were taken up into 4T1 cells after endocytosis. Therefore, loading of anticancer drugs in the MMS-NH₂-dsDNA complexes to deliver in cancer cells could significantly enhance the efficiency of drug delivery and magnetic hyperthermia, and thereby promote cancer therapy.

4. Conclusions

In this study, a temperature controlled release nanocarrier based on DNA-capped Fe₃O₄/SiO₂ magnetic mesoporous silica (MMS) nanoparticles has been developed. The results indicated that DOX, a model anticancer drug, was loaded in MMS nanoparticles and could be blocked by dsDNA through the hybridization of 15-mer ssDNA and 33-mer cDNA. DOX release could be controlled by the temperature-triggered denaturation of dsDNA capping agent. An in vitro study showed effective cell uptake of the MMS-NH₂-dsDNA complexes in murine breast cancer 4T1 cells, and negligible cytotoxicity of the MMS-NH₂-dsDNA complexes has been observed. Furthermore, MMS-NH₂ nanoparticles could efficiently generate heat upon exposure to an alternating magnetic field due to the superparamagnetic behavior. Therefore, DNA-capped MMS nanoparticles could be a promising multifunctional platform for potential cancer therapy with temperature controlled drug release and magnetic hyperthermia.

Acknowledgments

The authors gratefully acknowledge the support by the Program for Professor of Special Appointment (Eastern Scholar) at Shanghai Institutions of Higher Learning, National Natural Science Foundation of China (No. 51102166), Program for New Century Excellent Talent in University (No. NCET-12-1053), Shanghai Shuguang Project (No. 12SG39), Key Project of Chinese Ministry of Education (No. 212055) and the Huijiang Foundation of China (No. B14006).

References:

- [1] K. Cho, X. Wang, S. Nie, *Clin. Cancer Res.* 2008, 14, 1310-1316.
- [2] K. C.-W. Wu, Y.-H. Yang, Y.-H. Liang, H.-Y. Chen, E. Sung, Y. Yamauchi, F.-H. Lin, *Current NanoSci.* 2011, 7, 926-931.
- [3] M. Okada, T. Furuzono, *Sci. Technol. Adv. Mater.* 2012, 13, 064103 (14pp).
- [4] B. P. Bastakoti, Y.-C. Hsu, S.-H. Liao, K. C.-W. Wu, M. Inoue, S.-I. Yusa, K. Nakashima, Y. Yamauchi, *Chem. An Asian J.* 2013, 8, 1301-1305.
- [5] Y.-H. Yang, C.-H. Liu, Y.-H. Liang, F.-H. Lin, K. C.-W. Wu, *J. Mater. Chem. B*, 2013, 1, 2447-2450.
- [6] Z. Li, T. Wen, Y. Su, X. Wei, C. He, D. Wang, *CrystEngComm*, 2014, 16, 4202-4209.
- [7] I. I. Slowing, J. L. Vivero-Escoto, C. W. Wu, V. S. Y. Lin, *Adv. Drug. Delivery Rev.* 2008, 60, 1278-1288.
- [8] Q. He, J. Shi, *J. Mater. Chem.* 2011, 21, 5845-5855.
- [9] P. Yang, S. Gai, J. Lin, *Chem. Soc. Rev.* 2012,

- [10] C. Y. Lai, B. G. Trewyn, D. M. Jeftinija, K. Jeftinija, S. Xu, S. Jeftinija, V. S. Y. Lin, J. Am. Chem. Soc. 2003, 125, 4451-4459.
- [11] T. D. Nguyen, K. C. F. Leung, M. Liong, Y. Liu, J. F. Stoddart, J. I. Zink, Adv. Funct. Mater. 2007, 17, 2101-2110.
- [12] Y. Zhu, S. Kaskel, T. Ikoma, N. Hanagata, Micropor. Mesopor. Mater. 2009, 123, 107-112.
- [13] C. Park, K. Lee, C. Kim, Angew. Chem. Int. Ed. 2009, 48, 1275-1278.
- [14] Z. Luo, K. Y. Cai, Y. Hu, L. Zhao, P. Liu, L. Duan, W. H. Yang, Angew. Chem. Int. Ed. 2011, 50, 640-643.
- [15] Y. Zhu, W. Meng, H. Gao, N. Hanagata, J. Phys. Chem. C, 2011, 115, 13630-13636.
- [16] Z. Zou, D. G. e, X. X. He, K. M. Wang, X. Yang, Z. H. Qing, Q. Zhou, Langmuir, 2013, 29, 12804-12810.
- [17] Z. Zhang, D. Balogh, F. Wang, S. Y. Sung, R. Nechushtai, I. Willner, ACS Nano 2013, 7, 8455-8468.
- [18] P. Zhang, F. Cheng, R. Zhou, J. Cao, J. Li, C. Burda, Q. Min, J.-J. Zhu, Angew. Chem. Int. Ed. 2014, 53, 2371-2375.
- [19] Q. Fu, G. V. R. Rao, L. K. Ista, Y. Wu, B. P. Andrzejewski, L. A. Sklar, T. L. Ward, G. P. López, Adv. Mater. 2003, 15, 1262.
- [20] Z. Zhou, S. Zhu, D. Zhang, J. Mater. Chem. 2007, 17, 2428.
- [21] Y. You, K. K. Kalebaila, S. L. Brock, D. Oupický, Chem. Mater. 2008, 20, 3354.
- [22] Y. F. Jiao, Y. F. Sun, B. S> Chang, D. R. Lu, W. L. Yang, Chem. Eur. J. 2013, 19, 15410-15420.

- [23] E. Aznar, L. Mondragon, J. V. Ros-Lis, F. Sancenon, M. D. Marcos, R. Martinez-Manez, J. Soto, E. Perez-Paya, P. Amoros, *Angew. Chem. Int. Ed.* 2011, 50, 11172-11175.
- [24] J. Liu, C. Detrembleur, M.-C. De Pauw-Gillet, S. Mornet, L. V. Elst, S. Laurent, C. Jérôme, E. Duguet, *J. Mater. Chem. B* 2014, 2, 59-70.
- [25] Z. Yu, N. Li, P. Zheng, W. Pan, B. Tang, *Chem. Commun.* 2014, 50, 3494-3497.
- [26] C. Chen, F. Pu, Z. Huang, Z. Liu, J. Ren, X. Qu, *Nucleic Acids Res.* 2011, 39, 1638-1644.
- [27] A. Schlossbauer, S. Warncke, P. M. E. Gramlich, J. Kecht, A. Manetto, T. Carell, T. Bein, *Angew. Chem. Int. Ed.* 2010, 49, 4734-4737.
- [28] E. Climent, R. Martinez-Máñez, F. Sancenón, M.D. Marcos, J. Soto, A. Maquieira, P. Amorós, *Angew. Chem. Int. Ed.* 2010, 49, 7281-7283.
- [29] X. Ma, O. S. Ong, Y. Zhao, *Biomater. Sci.* 2013, 1, 912-917.
- [30] J. Yang, X. Liu, Z. Liu, F. Pu, J. S. Ren, X. G. Qu, *Adv. Mater.* 2012, 24, 2890-2895.
- [31] E. Ruiz-Hernandez, A. Baeza, M. Vallet-Regí, *ACS Nano*, 2011, 5, 1259-1266.
- [32] N. Li, Z. Yu, W. Pan, Y. Han, T. Zhang, B. Tang, *Adv. Funct. Mater.* 2013, 23, 2255-2262.
- [33] Y.-T. Chang, P.-Y. Liao, H.-S. Sheu, Y.-J. Tseng, F.-Y. Cheng, C.-S. Yeh, *Adv. Mater.* 2014, 24, 3309-3314.
- [34] Y. Zhu, W. Meng, N. Hanagata, *Dalton Trans.* 2011, 40, 10203-10208.
- [35] R. Jin, G. Wu, Z. Li, C. A. Mirkin, G. C. Schatz, *J. Am. Chem. Soc.* 2003, 125, 1643-1654.

- [36] J. Lammertyn, A. Peirs, J. De Baerdemaeker, B. Nicolai, *Postharvest Biol. Technol.* 2000, 18, 121-132.
- [37] M. H. Cho, E. J. Lee, M. Son, J.-H. Lee, D. Yoo, J. Kim, S. W. Park, J.-S. Shin, J. Cheon, *Nat. Mater.* 2012, 11, 1038-1043.
- [38] C. S. S. R. Kumar, F. Mohammad, *Adv. Drug. Delivery Rev.* 2011, 63, 789-808.
- [39] A. P. Khandhar, R. M. Ferguson, J. A. Simon, K. M. Krishnan, *J. Appl. Phys.* 2012, 111, 07B306
- [40] T.-C. Lin, F.-H. Lin, J.-C. Lin, *Acta Biomater.* 2012, 8, 2704-2711.
- [41] D. Yoo, H. Jeong, C. Preihs, J.-S. Choi, T.-H. Shin, J.-L. Sessler, J. Cheon, *Angew. Chem. Int. Ed.* 2012, 51, 12482-12485.
- [42] F. Lu, A. Popa, S. Zhou, J.-J. Zhu, A. C. S. Samia, *Chem. Commun.* 2013, 49, 11436-11438.
- [43] Y.-J. Kim, M. Ebara, T. Aoyagi, *Adv. Funct. Mater.* 2013, 23, 5753-5761.
- [44] C. D. Kowal, J. R. Bertino, *Cancer Res.* 1979, 39, 2285
- [45] C. Tao, Y. Zhu, *Dalton Trans.* 2014, 43, 15482-15490.
- [46] K. Zhang, L.-L. Xu, J.-G. Jiang, N. Calin, K.-F. Lam, S.-J. Zhang, H.-H. Wu, G.-D. Wu, B. Albela, L. Bonneviot, P. Wu, *J. Am. Chem. Soc.* 2013, 135, 2427-2430.
- [47] F. M. Martín-Saavedra, E. Ruíz-Hernández, A. Boré, D. Arcos, M. Vallet-Regí, N. Vilaboa, *Acta Biomater.* 2010, 6, 4522-4531.

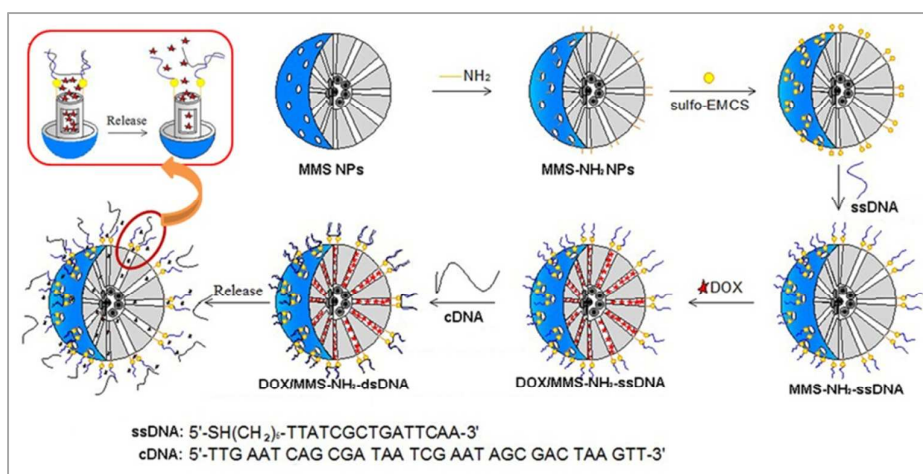


Fig. 1 Schematic illustration of preparation of temperature controlled drug release system based on DNA-capped Fe₃O₄/SiO₂ MMS nanoparticles.

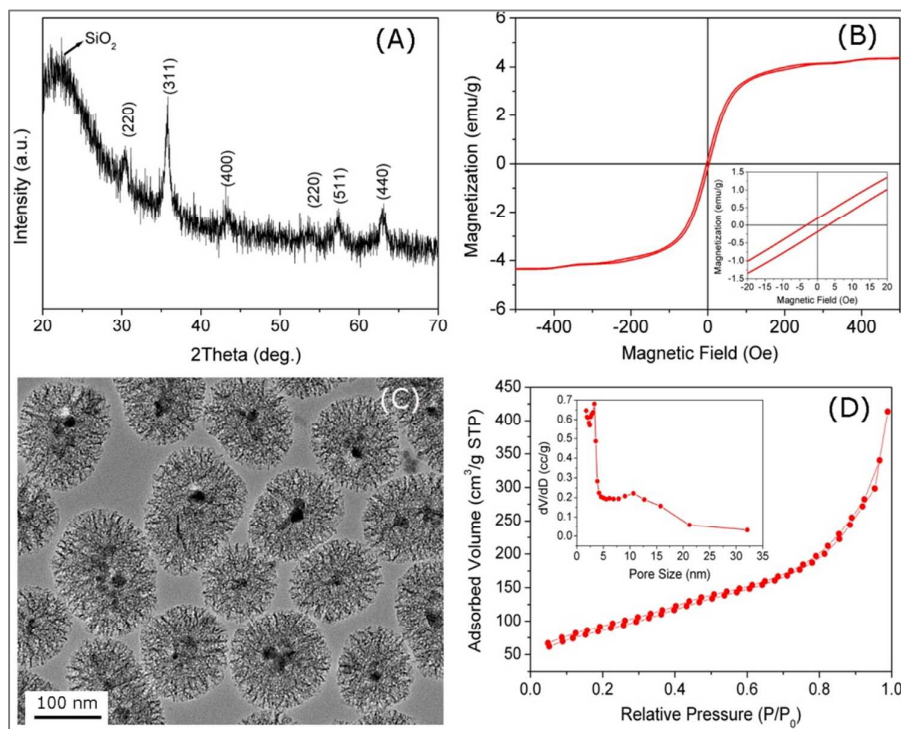


Fig. 2 (A) wide- angle XRD pattern, (B) magnetization curve measured at room temperature, (C) TEM image and (D) N₂ adsorption-desorption isotherm and the corresponding pore size distribution of MMS-NH₂ nanoparticles.

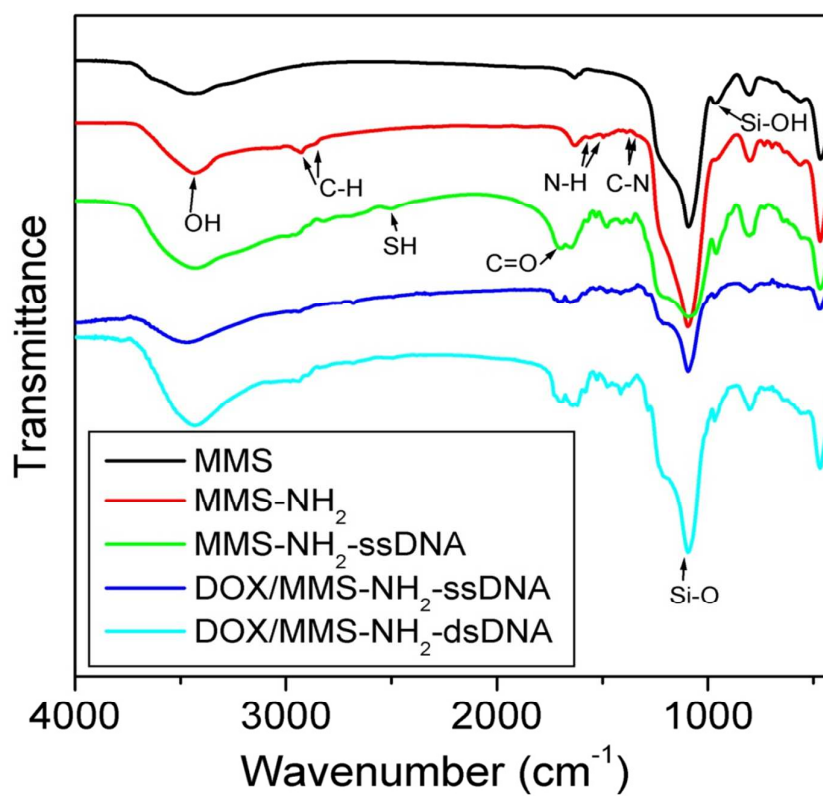


Fig. 3 FTIR spectra of MMS, MMS-NH₂, MMS-NH₂-ssDNA, DOX/MMS-NH₂-ssDNA and DOX/MMS-NH₂-dsDNA nanoparticles.

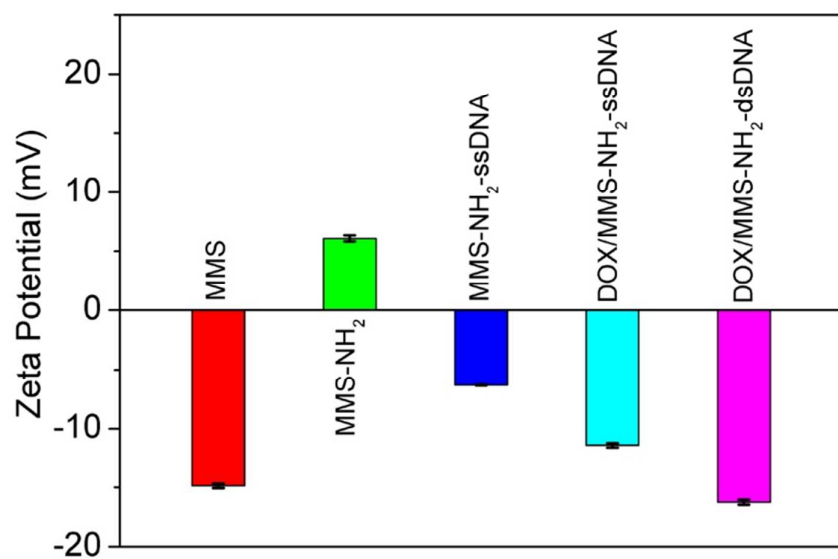


Fig. 4 Zeta potentials of MMS, MMS-NH₂, MMS-NH₂-ssDNA, DOX/MMS-NH₂-ssDNA and DOX/MMS-NH₂-dsDNA nanoparticles in H₂O.

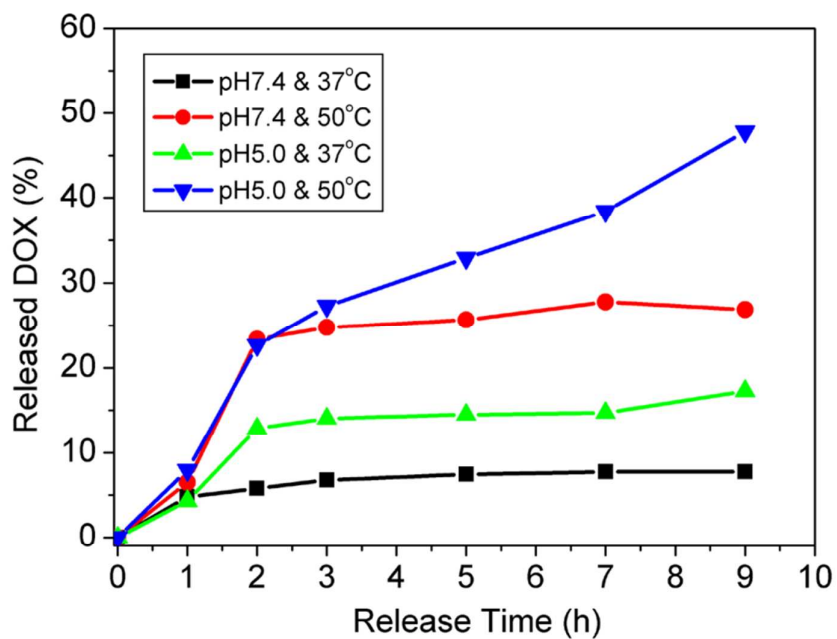


Fig. 5 The DOX release profiles of the DOX/MMS-NH₂-dsDNA complexes under different pH and temperature conditions.

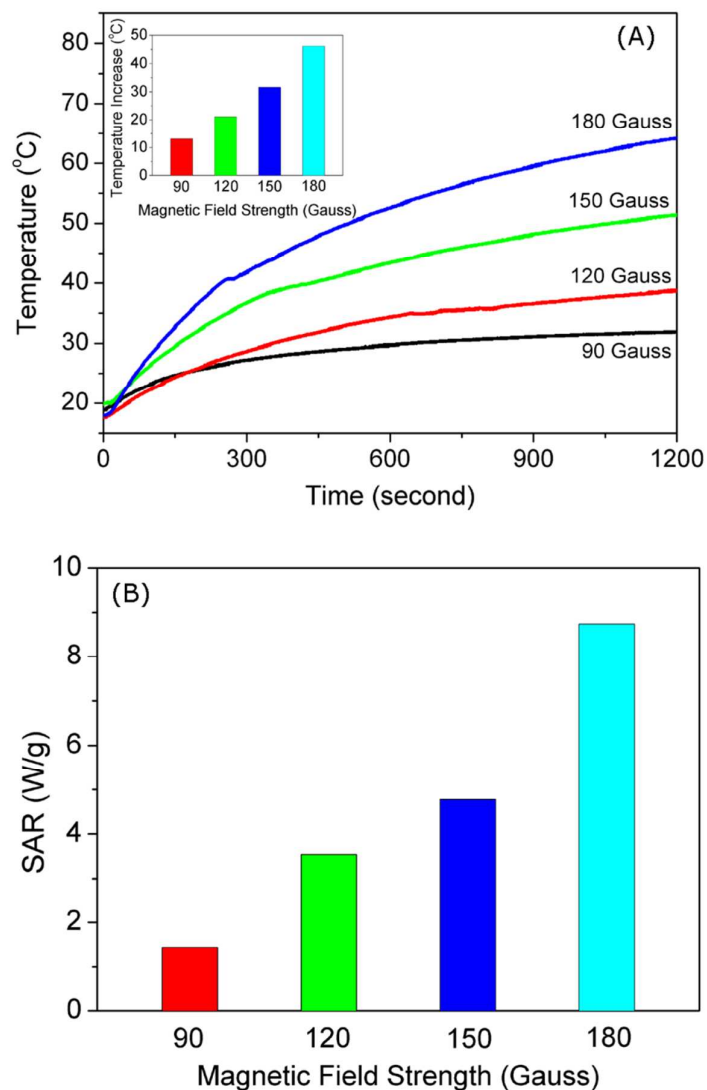


Fig. 6 The magnetic heating capacity of the MMS-NH₂ nanoparticles with a concentration of 50 mg/ml in H₂O evaluated under the magnetic field with a frequency of 409 kHz and magnetic field strength of 90-180 Gauss: (A) temperature kinetic curves; (B) the specific absorption rate (SAR) of the MMS-NH₂ nanoparticles under different magnetic field strength.

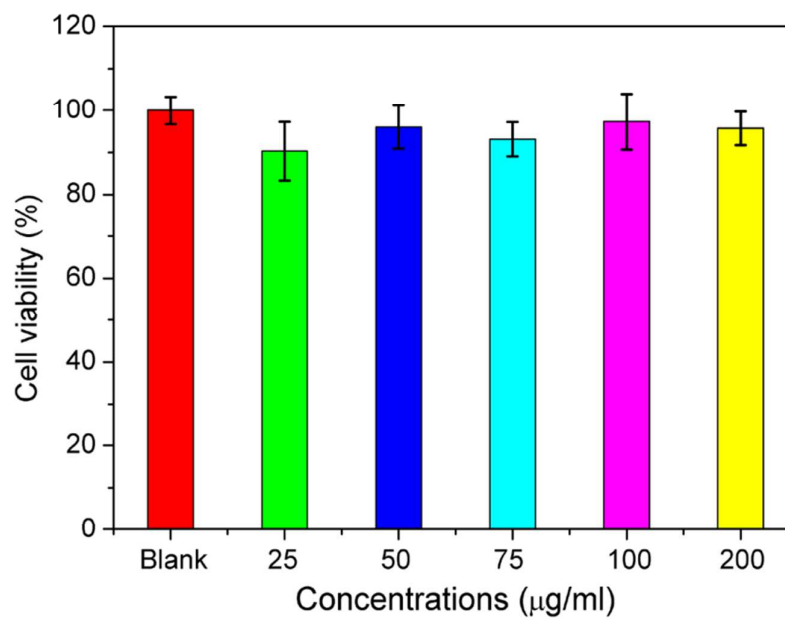


Fig. 7 In vitro cytotoxicity evaluation of the MMS-NH₂-dsDNA complexes to murine breast cancer 4T1 cells, as measured by MTT assay.

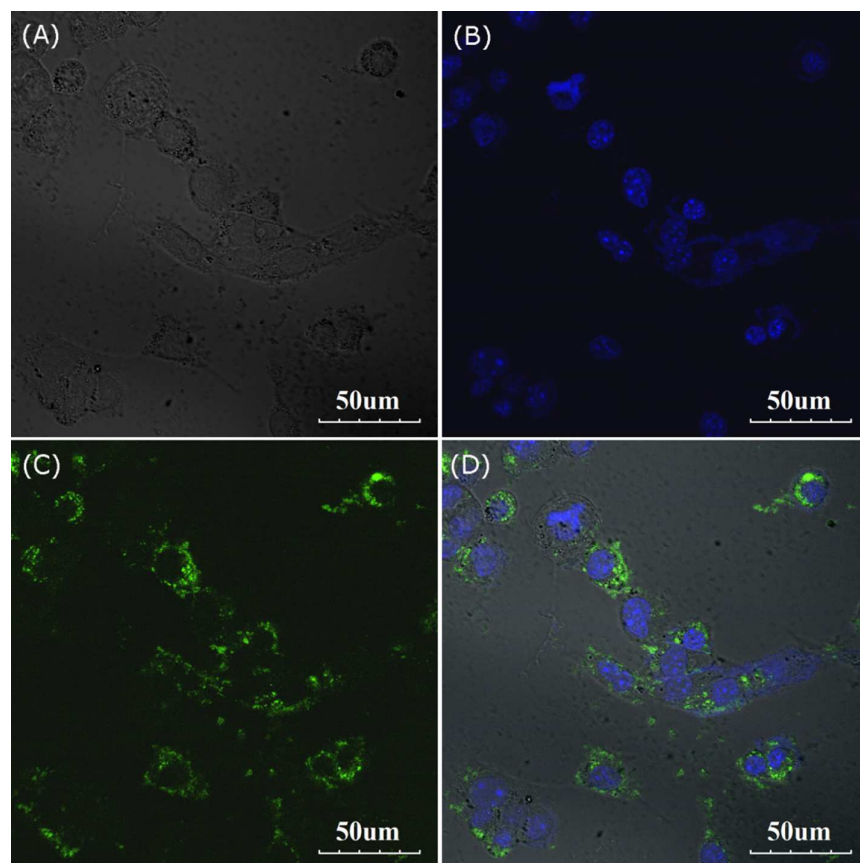


Fig. 8 Confocal laser scanning microscope (CLSM) images of 4T1 cells after 6 h of incubation with the MMS-NH₂-dsDNA-FITC complexes: (A) bright field; (B) DAPI channel; (C) FITC channel and (D) merged from bright, DAPI and FITC channels.